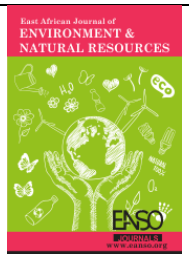

East African Journal of Environment and Natural Resources
eajenr.eanso.org
Volume 7, Issue 1, 2024
Print ISSN: 2707-4234 | Online ISSN: 2707-4242
Title DOI: https://doi.org/10.37284/2707-4242

EAST AFRICAN NATURE & SCIENCE ORGANIZATION

Original Article

Landslide Susceptibility Assessment Using Frequency Ratio: A Case Study of Kiliba (Sud-Kivu/DR Congo)

Isaac Chunga Chako[1], Toussaint Mugaruka Bibentyo[1], Guy Ilombe Mawe[1], Prof. Charles Nzolang, PhD[1], Prof. Majaliwa Mwanjalolo, PhD[2], Prof. Fils Makanzu Imwangana, PhD[3]*

[1] Official University of Bukavu, P. O. Box Bukavu, DR Congo.
[2] Makerere University, P. O. Box 7062, Kampala, Uganda.
[3] University of Kinshasa, P. O. Box 190 Kinshasa XI Lemba DR Congo.
[*] Correspondence ORCID: https://orcid.org/0000-0002-0793-7969; Email: chungachako@gmail.com

Article DOI: https://doi.org/10.37284/eajenr.7.1.2008

Date Published: *30 June 2024*

Keywords: *Landslide Susceptibility, Frequency Ratio, Uvira Territory, Deforestation, Risk Management.*

ABSTRACT

The conversion of natural ecosystems into agricultural or urban areas can alter geomorphological processes, particularly in landslide-prone regions. Landslides in such areas can be triggered by natural events like heavy rainfall or earthquakes, as well as human activities such as deforestation and unplanned urbanization. Their impacts can be severe, resulting in significant socio-economic damage. Uvira Territory, in the western part of the East African Rift Valley, frequently experiences these events. It is located between the Ruzizi Plain to the east and the Mitumba Mountains to the west, with diverse geology comprising precambrian formations and quaternary sediments. The topography has a stepped relief with altitudes ranging from 770 to 3250 meters. The climate is tropical and humid, with a rainy season from September to May and a dry season from June to August. The area features coastal plains and mountain slopes, with many waterways flowing into Lake Tanganyika or the Ruzizi River. Detailed studies on landslide susceptibility mapping in this area are limited. This study aimed to map landslide susceptibility in the Kiliba River catchment to assist policymakers in land management. It used Google Earth images, GPS surveys, and field observations, applying a Frequency Ratio (FR) model that considered seven geo-environmental factors: slope, aspect, elevation, distance to watercourses, topographic wetness index, vegetation cover, and land use/landcover. The inventory identified 106 landslides in the study area, with densities of up to 11.25 landslides per km². Key factors in predicting landslide susceptibility were slope, elevation, and vegetation cover. The prediction model had an accuracy rate of 72.2%. The study shows that regions at medium elevation with steep slopes and low vegetation cover are mostly at risk for landslides. These findings are key for land management and disaster prevention. Future studies should consider more factors and a broader geographic range to enhance risk management.

APA CITATION

Chako, I. C., Bibentyo, T. M., Mawe, G. I., Nzolang, C., Mwanjalolo, M. & Imwangana, F. M. (2024). Landslide Susceptibility Assessment Using Frequency Ratio: A Case Study of Kiliba (Sud-Kivu/DR Congo). *East African Journal of Environment and Natural Resources*, *7*(1), 183-199. https://doi.org/10.37284/eajenr.7.1.2008.

Article DOI: https://doi.org/10.37284/eajenr.7.1.2008

CHICAGO CITATION

Chako, Isaac Chunga, Toussaint Mugaruka Bibentyo, Guy Ilombe Mawe, Charles Nzolang, Majaliwa Mwanjalolo and Fils Makanzu Imwangana. 2024. "Landslide Susceptibility Assessment Using Frequency Ratio: A Case Study of Kiliba (Sud-Kivu/DR Congo)". *East African Journal of Environment and Natural Resources* 7 (1), 183-199. https://doi.org/10.37284/eajenr.7.1.2008.

HARVARD CITATION

Chako, I. C., Bibentyo, T. M., Mawe, G. I., Nzolang, C., Mwanjalolo, M. & Imwangana, F. M. (2024) "Landslide Susceptibility Assessment Using Frequency Ratio: A Case Study of Kiliba (Sud-Kivu/DR Congo)", *East African Journal of Environment and Natural Resources*, 7 (1), pp. 183-199. doi: 10.37284/eajenr.7.1.2008.

IEEE CITATION

I. C., Oloitipitip, T. M., Bibentyo, G. I., Mawe, C., Nzolang, M., Mwanjalolo, & F. M., Imwangana. "Landslide Susceptibility Assessment Using Frequency Ratio: A Case Study of Kiliba (Sud-Kivu/DR Congo)", *EAJENR*, vol. 7, no. 1, pp. 183-199, Jun. 2024. doi: 10.37284/eajenr.7.1.2008

MLA CITATION

Chako, Isaac Chunga, Toussaint Mugaruka Bibentyo, Guy Ilombe Mawe, Charles Nzolang, Majaliwa Mwanjalolo & Fils Makanzu Imwangana. "Landslide Susceptibility Assessment Using Frequency Ratio: A Case Study of Kiliba (Sud-Kivu/DR Congo)". *East African Journal of Environment and Natural Resources*, Vol. 7, no. 1, Jun 2024, pp. 183-199, doi:10.37284/eajenr.7.1.2008.

INTRODUCTION

In recent decades, natural disasters, including floods, earthquakes, wildfires, and landslides, have increased in frequency and intensity (Ozer, 2009). Landslides pose a significant hazard in numerous regions characterized by pronounced relief. Their consequences, contingent upon the scale and velocity of the processes, can precipitate into severe disruptions in societal structures. They incur loss of life and inflict structural and functional damage to infrastructure (Akter et al., 2018; Mugaruka, 2018). Furthermore, they engender disturbances to aquatic ecosystems in lakes through river siltation (Alin et al., 2002; Mölsä et al., 1999). In humid tropical regions, these disasters are often linked to intense rainfall, causing landslides that significantly impact local communities (Saley et al., 2005). The ramifications of landslides can transcend their immediate locale; they disrupt natural water drainage and alter sediment balances, leading to river siltation and potentially triggering flash floods (Gill and Malamud, 2014).

The Democratic Republic of the Congo (DRC) ranks among the countries most vulnerable to disasters from natural hazards stemming from gravitational movements. These disasters, on a national scale, rank as the second deadliest after volcanic eruptions between 1968 and 2003 (Maki and Dewitte, 2014). The western part of the East African Rift Valley, where the territory of Uvira is located, is one of the regions most affected by deadly landslides (Maki et al., 2016). The urban areas of Uvira, particularly its urban core, have borne the brunt of various natural disaster events in recent years, notably, floods attribute to landslides in the hills surrounding the city of Uvira and its environs (Azanga et al., 2016). Population growth and unplanned land use contribute to this vulnerability (Defries et al., 2010). Although the problem is serious, only a limited number of studies have explored landslide susceptibility mapping in this region. The works of Depicker et al. (2020) and Dewitte et al. (2021) are among the few that have addressed this topic in the East African Rift Valley. Our study aims to fill this gap by mapping the landslide susceptibility gradient in the eastern part of the Democratic Republic of Congo, with a particular focus on the Kiliba River catchment in the Uvira territory. Through this analysis, we hope to identify the most vulnerable areas and provide valuable data for land-use planning and risk management. The results will allow policymakers to develop strategies to minimize the risks associated with landslides and mitigate their devastating consequences.

STUDY AREA

The study area is part of the northwest basin of Lake Tanganyika in the western sub-catchment in of the Ruzizi River. It is located between 3°11'50'' and 3°19'19'' south latitude and 28°57'47'' and 29°12'38'' east longitude (*Figure 1*).

Article DOI: https://doi.org/10.37284/eajenr.7.1.2008

Figure 1: Location map of the study area.

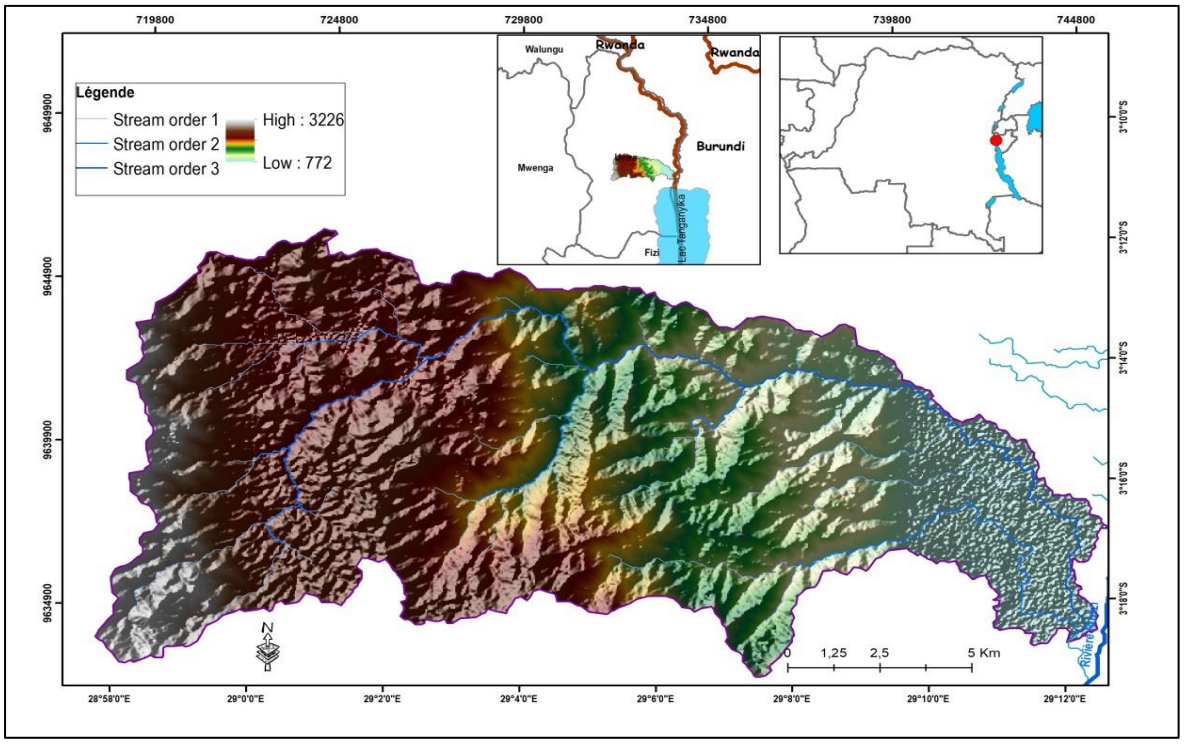

It is situated between the Ruzizi Plain (to the east) and the Mitumba Mountains (to the west), from which its watercourses originate. Its eastern boundary is marked by the Ruzizi River, which serves as its outlet. To the southeast, it is bounded by the city of Uvira. The altitude ranges from 770 meters to 3250 meters.

The territory of Uvira, located in the western branch of the East African Rift Valley, features a geography characterized by a stepped relief formed by a succession of horsts and grabens The landscape consists of two main geomorphological components: the coastal plain and the eastern slope of the Mitumba Mountains (Ilunga, 1991). This region encompasses the Kiliba catchment, traversed by many small rivers, some permanent and others temporary, which either flow into Lake Tanganyika or the Ruzizi River after descending longitudinal slopes of 10 to 12% (Ilunga, 2006). The geology of the territory is based on precambrian formations that are folded and metamorphosed, consisting of gneiss, quartzites, mica schists, amphibolite, schists, granites, along with quaternary formations containing old sandy-gravelly alluvium (Ilunga, 1991). The Paleozoic formations primarily occupy the mountainous area, while Quaternary sediments are located in the plain, creating a diverse and complex geological landscape (Nacishali, 2021a).The region has a humid tropical climate characterized by the alternation of two unequal seasons: a rainy season from September to May and a dry season from June to August. Annual precipitation varies between 868 mm and 2041 mm, with an average of 1525 mm. In the city of Uvira, precipitation is less than 1000 mm, but with increasing altitude, precipitation ranges from 1000 to 2000 mm in the high plateaus in the central and western regions (Nacishali, 2021b). The average annual temperature is 24°C, and the maximum temperature in the Lake Tanganyika valley almost always exceeds 25°C on average throughout the year. The minimum temperature remains above or equal to 20°C every three days. The wind is generally from the south and very low to the ground during the night and morning, strengthening in the afternoon (Azanga et al., 2016; Nacishali, 2021b).

MATERIAL AND METHODS

Landslide Inventory

Article DOI: https://doi.org/10.37284/eajenr.7.1.2008

A higher resolution of images across the entire study area can facilitate the detection of landslides more easily, especially in sectors where landslides are rare (Maki and Dewitte, 2014). Landslides were initially identified on Google Earth images, and for each identified landslide, a point was placed with an identity. The landslides were then digitized into polygons. The layer in KML format containing all landslides was created, saved, and then imported into ArcGIS to be converted into a vector (shapefile) format. Due to the scarcity or very limited number of available images in the study area, the temporal aspect or age of landslides was not considered (the age of landslides was not regarded as a variable or parameter). The use of Google Earth in this study is justified by its ability to provide high-resolution images covering the entire study area, facilitating the precise and efficient identification of landslides even in sectors where they are rare, as well as by the capability to visualize inaccessible areas and reduce the costs and logistical efforts associated with traditional field studies (Mugaruka, 2018).

To present the inventory of landslides (sampling), centroids of these landslides were generated in ArcGIS. The density of landslide centroid points in an area represents the spatial distribution of landslides; it illustrates the unequal spatial distribution (Maki and Dewitte, 2014). To achieve this, the "Kernel Density" tool in the spatial analysis of ArcGIS software will be used. This tool calculates a magnitude per unit area from point or polyline features using a Kernel function to fit a slightly tapered surface to each point or polyline.

Landslide Causative Factor

Slope

The inclination of the terrain significantly influences the spatial distribution and severity of landslides (Du et al., 2017; Khan et al., 2019; Shafique et al., 2016). The variability in terrain steepness was assessed using the ASTER Digital Elevation Model (DEM) in ArcGIS 10.5, employing a moving window technique based on the methodology proposed by Khan et al. (2019). The slope gradient was divided into 5 distinct categories: Very weak: 0 to 10°; Weak: 10 to 18°; Mean: 18 to 25°; High: 25 to 32°; Very high: 32 to 66°.

Slope Aspect

The aspect of slope is influenced by various factors such as sunlight exposure, precipitation, wind impact, land use, and orientation of discontinuities (Guo et al., 2015; Xu et al., 2012), all of which are associated with landslide occurrence. The slope orientation classes were divided into 8 categories as follows: N (0-29 and >327); NE (29-68); E (68-106); SE (106-145); S (145-188); SW (188-235); W (235-282); NW (282-327).

Elevation

Elevation is a significant factor influencing the occurrence of landslides. It is interconnected with other factors such as precipitation, soil types, vegetation types, and vegetation cover. Several researchers utilize elevation as a factor in developing landslide susceptibility maps (Dai and Lee, 2003; Du et al., 2017; Hong et al., 2015; Park, 2011; Yalcin et al., 2011; Yilmaz, 2010). In this study, elevation variations were categorized into 5 classes as follows: Very low elevation: 772-1100 m; Low elevation: 1000-1500 m; Moderate elevation: 1500-2000 m; High elevation: 2000-2500 m; Very high elevation: > 2500 m.

Proximity to Drainage

To assess the impact of watercourses on the distribution of landslides, the hydrographic network of the study area was delineated from the ASTER DEM using the ArcHydro tools in ArcGIS. Distances from the drainage network were divided into 5 buffers as follows: Very close: 0 to 74 m; Close: 74 to 155 m; Moderately close: 155 to 244 m; Distant: 244 to 355 m; Very distant : 355 to 500 m.

Vegetation Cover

Generally, it has been demonstrated that a higher vegetation cover leads to a reduced frequency of landslides (Du et al., 2017). Vegetation cover was derived from Landsat 8 images using the image analysis tool in ArcGIS software. The vegetation

Article DOI: https://doi.org/10.37284/eajenr.7.1.2008

cover was calculated using equation (1) (Xiao & Moody, 2005) : NDVI = (IR - R) / (IR + R) (1). Where NDVI stands for Normalized Difference Vegetation Index, IR represents the near-infrared part of the electromagnetic spectrum, and R represents the red part of the electromagnetic spectrum. In this study, Landsat 8 images were utilized, with IR corresponding to the 5th band and R corresponding to the 4th band.

Topographic Wetness Index (TWI)

The Topographic Wetness Index (TWI) is a function of both slope and contributing area per unit orthogonal width to the flow direction. It is commonly used to quantify the topographic control of hydrological processes (Park et al., 2013; Roy and Saha, 2019). The TWI thematic layer was prepared from ASTER DEM images in a GIS environment using the following equation (2) from Moore (1978), Roy and Saha, (2019) : TWI = ln (α / (Tanβ + C)) (2).

Where TWI represents the Topographic Wetness Index, α is the cumulative upslope contributing area passing through a point (per unit contour length), β is the slope gradient (in degrees), and C = 0.001.

The equation will be processed in the ArcGIS software, and calculations will be performed using the Raster Calculator tool in the Spatial Analysis menu as follows:

TWI = ln ((α + 1) * Cell size) / (Tan (β * π/180) + 0.001) (3).

The π/180 ratio is used to convert the slope from degrees to radians (handled by the Raster Calculator). In this formula, Cell size represents the pixel size.

Land Use/Land Cover

Supervised classification of Landsat 8 images was conducted using the image analysis tool in ArcGIS software. The year 2016 was chosen as the only period with complete images in the Kiliba catchment. The classification considered 5 land use/land cover classes: agricultural land and grassland, residential areas, bare soil, woodland, and water bodies. For classification, pixel sampling for land use was performed using Google Earth imagery, supplemented by field data. Sampling was conducted beyond the catchment, and the generated raster was then clipped according to the catchment boundary. After classification, the confusion matrix was generated, and the Kappa index was derived to verify the accuracy of the classification (Azanga et al., 2016). Similar to NDVI, the Landsat images used were from November 26, 2015 (rainy season).

Mapping Landslide Susceptibility

Frequency Ratio (FR) model

Several studies have used the Frequency Ratio (FR) approach to assess landslide susceptibility (Hidayat et al., 2019; Park et al., 2013; Rabby and Li, 2020; Silalahi et al., 2019; Solaimani et al., 2013). It is based on observation for the preparation of general landslide susceptibility maps. The FR value for each class can be calculated using Equation 4:

$$FR_j = \frac{Nij/Ntotal}{Aij/Atotal} \quad (4)$$

Where, Nij = the number of landslide pixels in the j_{th} subclass of factor i; N_{total} = the total number of landslide pixels in the study area; A_{ij} = the total number of pixels in the j_{th} subclass of factor i; A_{total} = the total number of pixels in the study area.

The distribution and frequency ratio analyses were not conducted while considering portions of the study area where landslide occurrences are impossible (Mugaruka, 2018); that is, the surface covered by flat land and water bodies. After determining the FR values for all classes of each factor, a Landslide Susceptibility Index (LSI) was derived and applied in the GIS by summing up the FR values of all factors according to Equation (5):

$$LSI = FR_1 + FR_2 + FR_3 + \ldots + FR_n \quad (5)$$

Where, LSI = the landslide susceptibility index at each pixel in the study area; FR = the frequency ratio of each factor class at the pixel; n = the total number of factors.

Validation of the Prediction Model Using the AUC Approach

Article DOI: https://doi.org/10.37284/eajenr.7.1.2008

All conditioning factors were evaluated using the Area Under Curve (AUC) approach. AUC is a type of statistical accuracy for prediction models (probabilities) in the assessment or analysis of natural disaster occurrences. The AUC value defines conditioning factors that would be used in landslide susceptibility mapping using the FR method. The higher the AUC value (if the threshold definition achieves the maximum value of 1), the higher the statistical accuracy of the model, which describes the prediction threshold independently (Lepore et al., 2012; Mandal and Mandal, 2018; Mohammady et al., 2012; Pimiento, 2010; Rossi and Reichenbach, 2016; Silalahi et al., 2019; Xu et al., 2012; Yilmaz, 2010). The AUC curve was plotted with the cumulative percentages of predicted landslides (on the x-axis) and the cumulative percentages of observed landslides (on the y-axis).

RESULTS

Landslide Inventory

The density map effectively illustrates the inequality in the spatial distribution of landslides (*Figure 2*). A total of 106 landslides were inventoried, with 75% utilized in the model and 25% in model validation. The spatial distribution shows densities ranging from 0 to 11.25 landslides per km², with an average of 1.9 landslides per km². Considering the number of pixels per landslide density class exceeding 0.5 landslides per km², it is found that the highest density class, 8 to 11.5 landslides per km², represents a proportion of 5.1%, while the lowest density class, 0.5 to 1.5 landslides per km², represents a proportion of 55.6%.

Figure 2: Landslide density

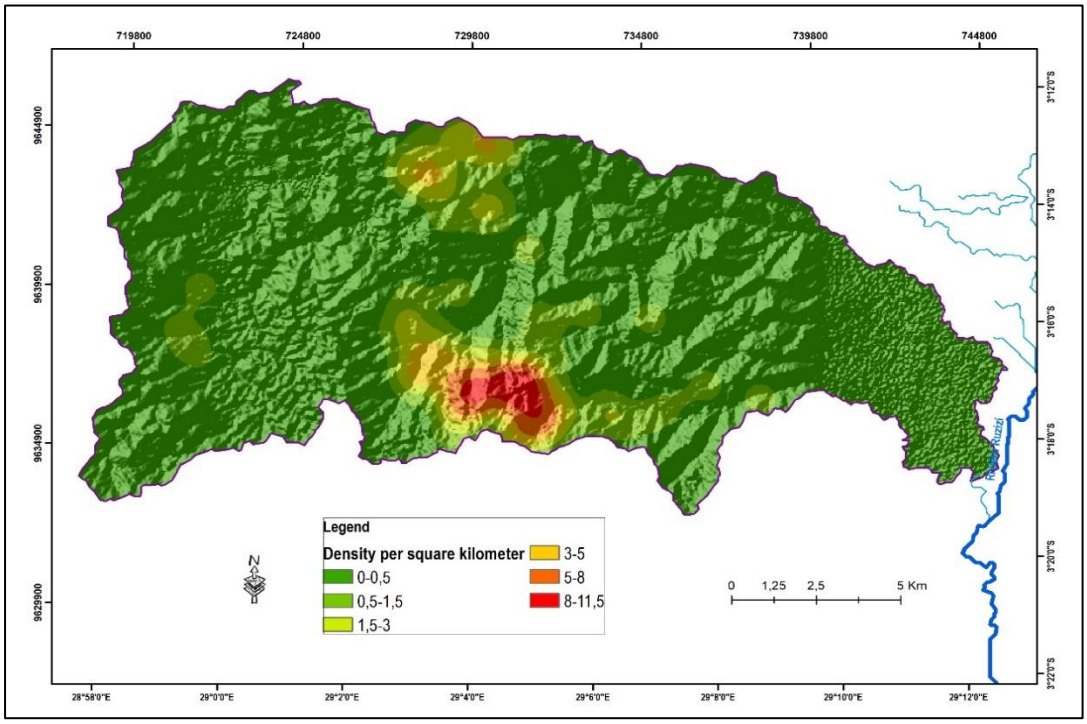

From a spatial distribution standpoint, landslides are more concentrated towards the southern part of the catchment, with the highest density reaching up to 11.25 landslides per km², followed by the northern part where the density is relatively moderate, reaching up to 3 landslides per km². Landslides are rare towards the western part, which cannot exceed 1 landslide per km², while the density becomes zero towards the eastern part as it is occupied by the Ruzizi plain.

Spatial Analysis of Landslide Distribution According to Different Classes within the Factors

The distribution of landslides according to slope classes shows the maximum value in the high

Article DOI: https://doi.org/10.37284/eajenr.7.1.2008

slope class, accounting for 36.9% of the total triggering area for landslides. The intersection of the curve, indicating the critical threshold of the slope which lies beyond 25° (*Figure 3a*). This threshold is the angle beyond which the landslide frequency increases while the slope of the study area decreases (Larsen and Montgomery, 2012; Mugaruka, 2018). The distribution of landslides according to slope aspect shows a predominance along the NW-SE orientation. This means that the majority of landslide triggering areas are located on NW-facing slopes, accounting for 23.6% of the total area, and SE-facing slopes, accounting for 20.6% of the total area (*Figure 3b*).

The critical threshold lies beyond the "low altitude" class, i.e., beyond 1500 m altitude. The mode of the distribution belongs to the "medium altitude" class, accounting for 49.8% of the total triggering areas for landslides. The "High altitude" class also holds a proportion close to the mode (45.9%), indicating that the two classes (medium and high altitudes) alone hold over 95% of the triggering area for landslides (*Figure 3c*). The majority (32.2%) of these landslides (their triggering areas) are located at a distance between 155 and 244 m from a drainage channel and on bare terrain (54% of the total triggering area), (*Figure 3d*). For the topographic wetness index (TWI), the highest proportion of landslides is located in the 2.284-5.048 class, accounting for 43.8%. The frequency of landslides as well as the area of TWI classes decrease together, becoming null in the last class (*Figure 3e*). The critical threshold for triggering in relation to the NDVI index is approximately 0.18 (*Figure 3f*), belonging to the same class as the peak of the triggering area distribution. This indicates a strong correlation between landslide frequency in the triggering area and in the non-triggering area. Landslides are rare in forested and built-up areas (*Figure 3g).*

Frequency Ratios of Landslides in Different Classes

Classes with a frequency ratio (FR) greater than 1 are susceptible to landslides (Kannan et al., 2013; Kirschbaum et al., 2012; Lee and Pradhan, 2007; Mugaruka, 2018). Thus, referring to the critical FR value, susceptibility in relation to slope begins to manifest from slopes exceeding 25°, without showing a decrease until reaching the maximum slope of the catchment. As slopes become steeper, the frequency ratios become higher (*Figure 4a*).

Therefore, the catchment is more susceptible to landslides in the classes of steep and very steep slopes, while noting that moderate slopes also exhibit frequencies close to the threshold. Regarding slope aspect, NW-facing slopes show a higher susceptibility than all other aspects, with FR values well above the critical threshold (*Figure 4b*). Susceptibility related to altitude remains concentrated between high altitudes and the upper limit of low altitude. The highest FR values are found in the medium altitude range. At low and very high altitudes, FR values are nearly zero (*Figure 4c*). Susceptibility appears from 155 m from a drainage channel onwards.

Comparing the distribution graph in landslide triggering areas/non-triggering areas with that of frequency ratios related to distance to drainage, it can be observed that landslides are rare in the 355-499 m class despite having the highest frequency ratio value (*Figure 4d*).The topographic wetness index presents FR values mostly below the critical threshold. Only one class has a value exceeding the threshold and with an FR very close to 1 (*Figure 4e*). For NDVI, the highest FR values are located where NDVI is lower. The peak is found in the 0-10% NDVI class, and values decrease with increasing NDVI. FR values remain almost identical and close to the critical threshold (1) in locations with NDVI greater than 10% up to 25%, before falling below 1. Locations with NDVI exceeding 25% and 50% are not susceptible to landslides as FR values are almost zero (*Figure 4f*). Only soils affected by agriculture and grassy vegetation, as well as bare land, exhibit susceptibilities exceeding the threshold (*Figure 4g*).

Article DOI: https://doi.org/10.37284/eajenr.7.1.2008

Figure 3: Distribution of factors in the study area (non-landslide zone) and in landslides (landslide zone): a: slope; b: slope orientation; c: altitude; d: distance to drainage; e: topographic wetness index; f: NDVI (Normalized Difference Vegetation Index); g: land use

a

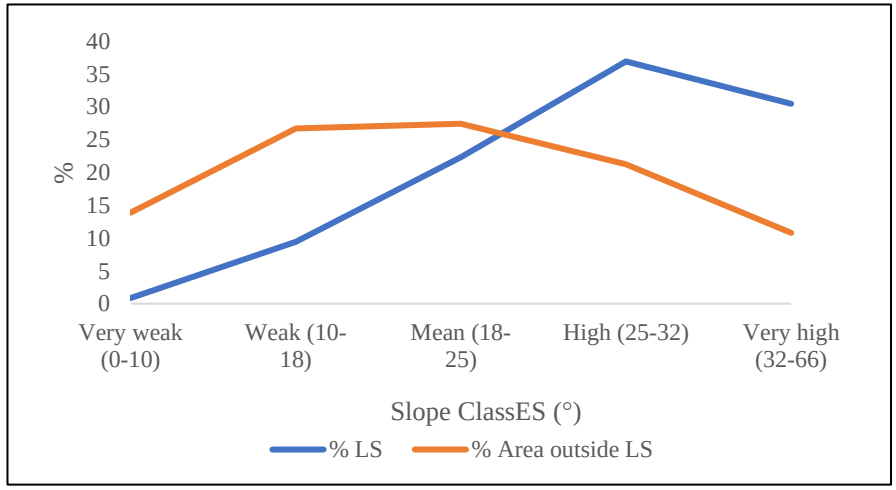

b

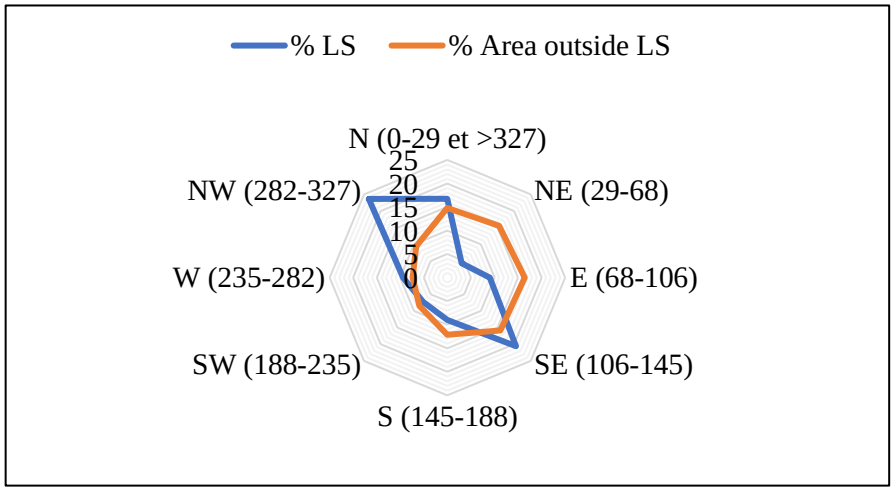

c

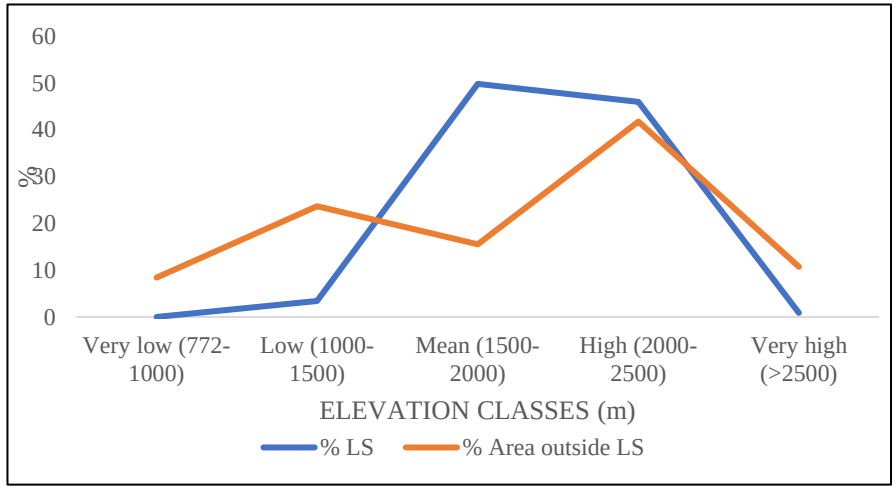

d

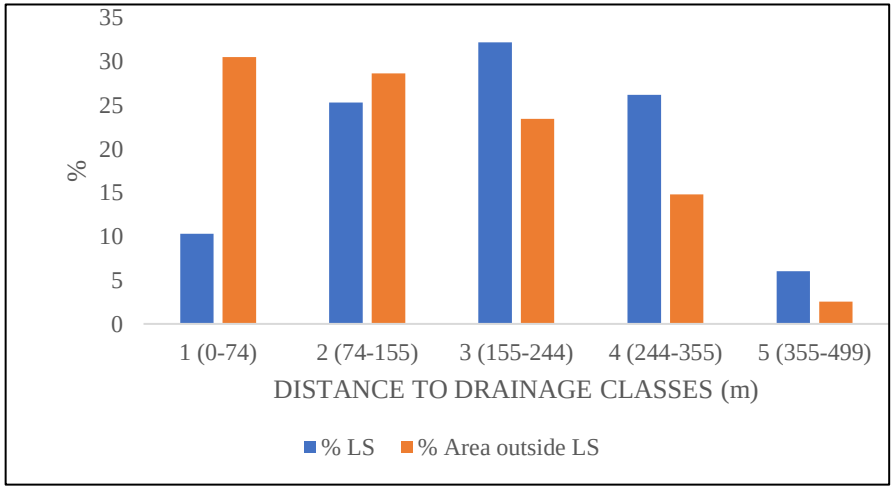

Article DOI: https://doi.org/10.37284/eajenr.7.1.2008

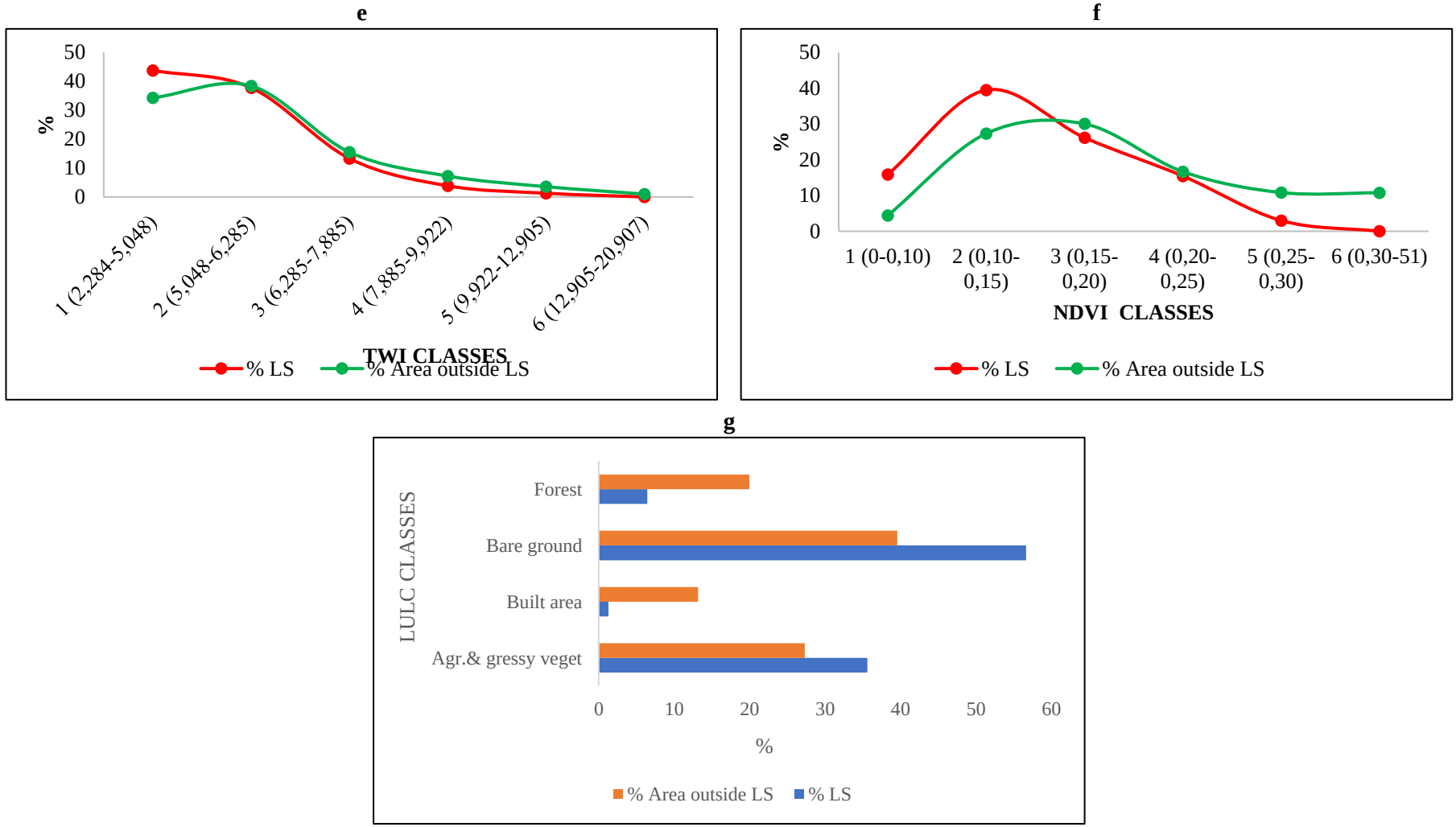

Article DOI: https://doi.org/10.37284/eajenr.7.1.2008

Figure 4: Distribution of frequency ratios (FR) of landslides in the various classes of factors: a: slopes; b: slope orientation; c: altitude; d: distance to drainage; e: topographic wetness index; f: NDVI; g: land use

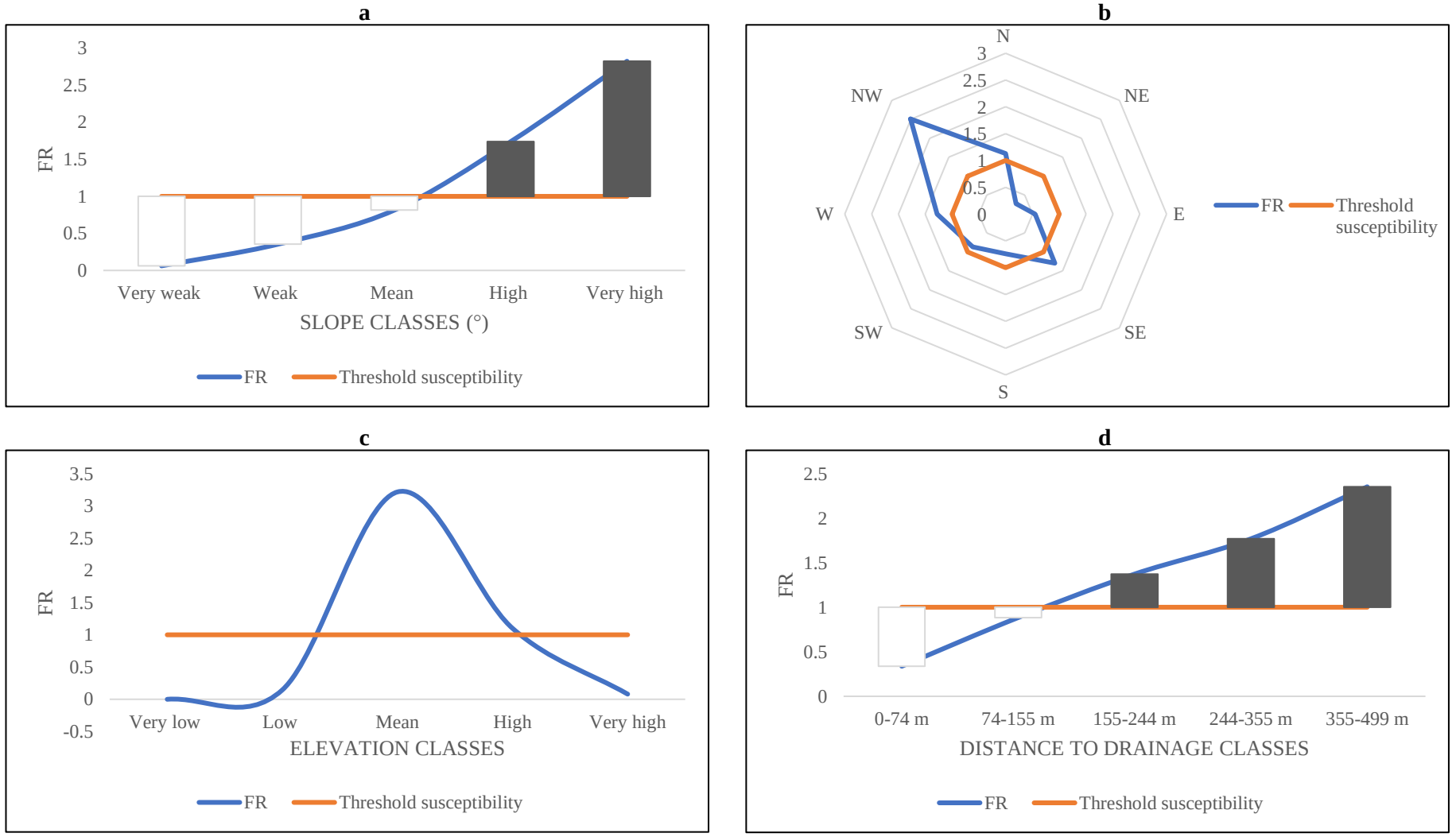

East African Journal of Environment and Natural Resources, Volume 7, Issue 1, 2024
Article DOI: https://doi.org/10.37284/eajenr.7.1.2008

e

f

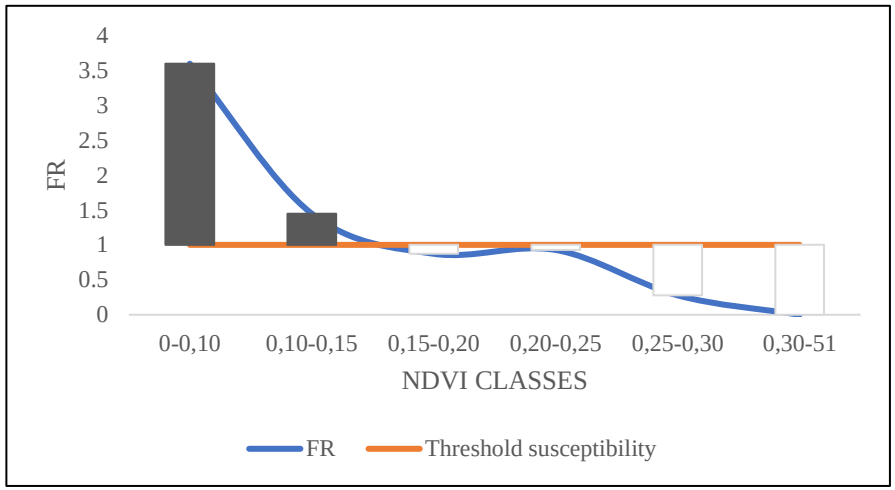

g

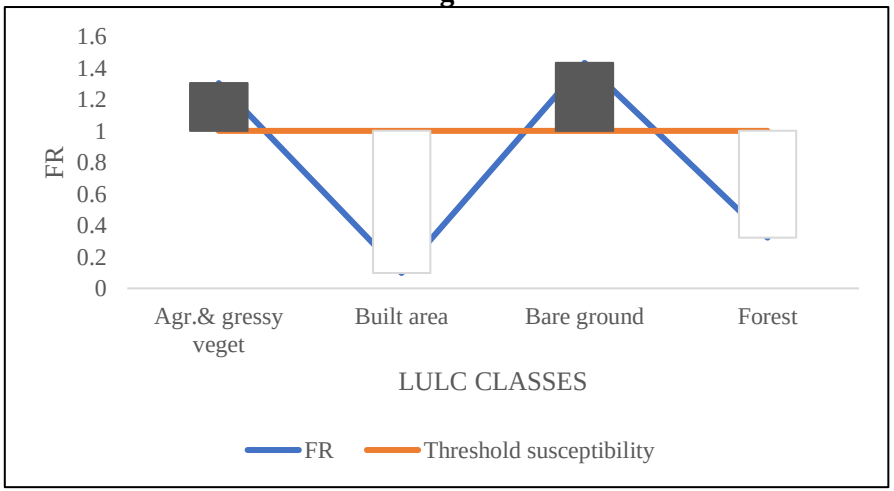

Article DOI: https://doi.org/10.37284/eajenr.7.1.2008

Landslide Susceptibility Index and Model Validation

The landslide susceptibility index (LSI) gradient indicates a variation from 0 to 14. It has been reclassified and subdivided into 5 susceptibility classes (levels) as follows (*Figure 5*): Very Low: 0 to 3; Low: 3-5; Moderate: 5-7; High: 7 to 9; Very High: 9 to 14. Model validation using the AUC approach indicates a reliability level of 0.7219, which corresponds to 72.2% accuracy in prediction (*Figure 6*).

Figure 5: Susceptibility to the landslide in the Kiliba catchment claimed according to the different LSI levels

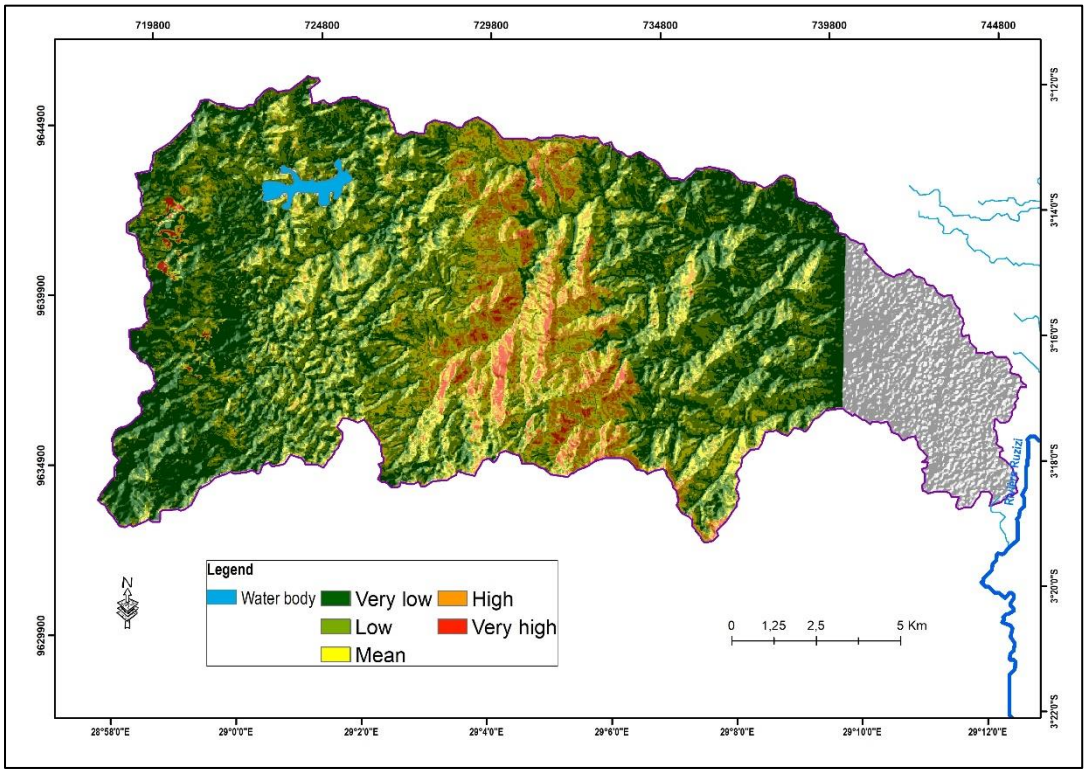

Figure 6: Validation curve according to the AUC approach, with the model reliability of 72.2%

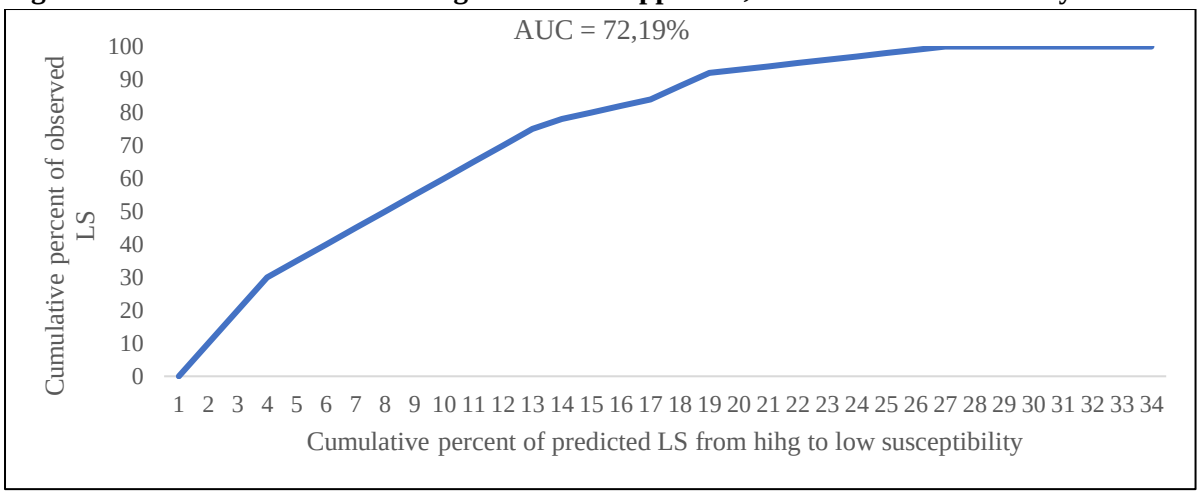

DISCUSSION

The information obtained from the landslide inventory reveals a density ranging from 0 to 11.25 landslides per square kilometre. These figures exceed those reported by Maki and Dewitte (2014), which range from 0 to 7.2 landslides per square kilometre, as well as those of Mugaruka (2018), which have an average of 1.6 landslides per square kilometre, a value

Article DOI: https://doi.org/10.37284/eajenr.7.1.2008

considered lower than that of Jacobs et al. (2017). Examination of the slopes of the hillsides where landslides occur reveals a critical threshold around 25°. This value differs from that found by Mugaruka (2018) in the catchment of Ruzizi River (18.9°), but is similar to that found by Maki and Dewitte (2014) in the western rift of Lake Kivu (25°) and higher than that found by Migombano (2011) in Bukavu. This value is consistent with the findings of Persichillo et al. (2017), showing that slopes greater than 25°, combined with socio-economic factors, are major triggers of landslides in Italy.

Regarding altitude, susceptibility begins to manifest itself from the upper limit of the low-altitude class (about 1500 m), remains high at middle altitudes, and decreases at high altitudes around 2500 m. The steep slopes at middle altitudes, associated with a higher drainage density, explain this prevalence. The altitude-triggered thresholds in the Kiliba catchment, found by Mugaruka (2018) almost coincide with these observations. Regarding land use, landslides are more frequent on bare soil, thens on soil covered with grass and cultivated vegetation.

Spatial analysis of the landslide susceptibility map shows a correlation between slope, altitude, NDVI, land cover, and landslide susceptibility. Landslides are sensitive to slope, soil exposure, and low NDVI values. Furthermore, the middle altitude class exhibits steeper slopes, a high proportion of bare soil, and grassland and cultivated vegetation (*Figure 7*).

Figure 7: Landslides in the Kiliba catchment: located on steep slopes, in the middle altitude class, in the land class affected by grassland and agriculture.

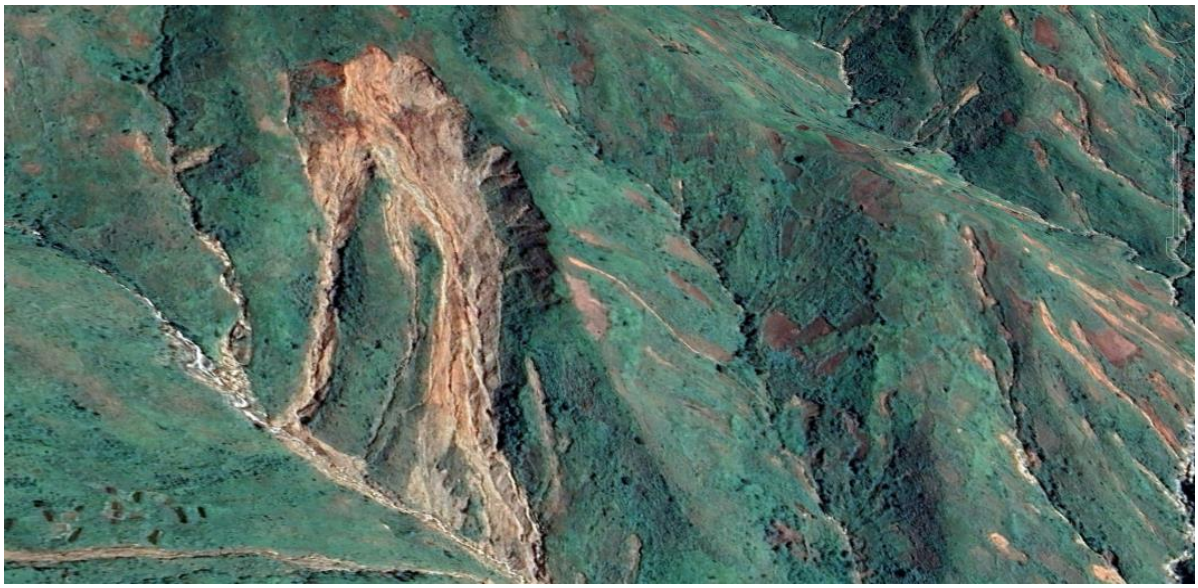

This observation aligns well with that made by Broothaerts et al.(2012), who demonstrated that deforestation for agricultural purposes and the transition from subsistence farming to intensive agriculture have led to landslide risks in the catchment of Gilgel Gibe catchment in southwest Ethiopia, as these activities destabilize the land surface. Similar observations were made in populated areas of Uganda by Knapen et al. (2006) who showed that agriculture, as the primary land use class, is one of the main factors influencing landslide risks. The results of the research conducted by (Zamukulu, 2020) on Idjwi Island showed similarity with the findings in the catchment of Kiliba catchment, our study area. It was found that in the island territory of Idjwi, areas occupied by fields and bare soil are most susceptible to landslides.

CONCLUSION

The study conducted in the catchment of Kiliba catchment identified landslide susceptibility factors. The results revealed an uneven spatial distribution of landslides, with a higher

Article DOI: https://doi.org/10.37284/eajenr.7.1.2008

concentration in the southern part of the catchment, on steep slopes and at moderate altitudes. The correlation between slope, altitude, NDVI, and land cover was highlighted, emphasizing the importance of these variables in landslide susceptibility modelling. Critical landslide triggering thresholds were identified, notably a slope greater than 25° and moderate altitudes around 1500 m. These thresholds corresponded to those found in other similar studies conducted in geographically comparable regions. Additionally, the impact of human activity, particularly agriculture and deforestation, on increasing landslide risks was emphasized, consistent with previous observations in other areas. Finally, validation of the susceptibility model showed acceptable accuracy, with a reliability level of 72.2%, reinforcing the robustness of the results. These conclusions provide important information for landslide risk management in the catchment of Kiliba catchment, highlighting the most vulnerable areas and identifying key factors to consider in mitigation and prevention strategies.

REFERENCES

Akter, T., Quevauviller, P., Eisenreich, S. J., & Vaes, G. (2018). Impacts of climate and land use changes on flood risk management for the Schijn River, Belgium. *Environmental Science and Policy*, *89*(July), 163–175. https://doi.org/10.1016/j.envsci.2018.07.002

Alin, S. R., O'Reilly, C. M., Cohen, A. S., Dettman, D. L., Palacios-Fest, M. R., & McKee, B. A. (2002). Effects of land-use change on aquatic biodiversity: A view from the paleorecord at Lake Tanganyika, East Africa. *Geology*, *30*(12), 1143–1146. https://doi.org/10.1130/0091-7613(2002)030<1143:EOLUCO>2.0.CO;2

Azanga, E., Majaliwa, M., Kansiime, F., Mushagalusa, N., Karume, K., & Tenywa, M. M. (2016). Land-use and land cover, sediment and nutrient hotspot areas changes in Lake Tanganyika Basin. *African Journal of Rural Development*, *1*(1), 75–90.

Broothaerts, N., Kissi, E., Poesen, J., Van Rompaey, A., Getahun, K., Van Ranst, E., & Diels, J. (2012). Spatial patterns, causes and consequences of landslides in the Gilgel Gibe catchment, SW Ethiopia. *Catena*, *97*, 127–136. https://doi.org/10.1016/j.catena.2012.05.011

Burrough, P. A., & McDonell. (1986). Principles of geographical. In *Information systems for land resource assessment …*. https://www.academia.edu/download/2438559/9fjg8q78n4wux4l.pdf

Dai, F. C., & Lee, C. F. (2003). A spatiotemporal probabilistic modelling of storm-induced shallow landsliding using aerial photographs and logistic regression. *Earth Surface Processes and Landforms*, *28*(5), 527–545. https://doi.org/10.1002/esp.456

Defries, R. S., Rudel, T., Uriarte, M., & Hansen, M. (2010). Deforestation driven by urban population growth and agricultural trade in the twenty-first century. *Nature Geoscience*, *3*(3), 178–181. https://doi.org/10.1038/ngeo756

Depicker, A., Jacobs, L., Delvaux, D., Havenith, H. B., Maki Mateso, J. C., Govers, G., & Dewitte, O. (2020). The added value of a regional landslide susceptibility assessment: The western branch of the East African Rift. *Geomorphology*, *353*, 106886. https://doi.org/10.1016/j.geomorph.2019.106886

Dewitte, O., Dille, A., Depicker, A., Kubwimana, D., Maki Mateso, J. C., Mugaruka Bibentyo, T., Uwihirwe, J., & Monsieurs, E. (2021). Constraining landslide timing in a data-scarce context: from recent to very old processes in the tropical environment of the North Tanganyika-Kivu Rift region. *Landslides*, *18*(1), 161–177. https://doi.org/10.1007/s10346-020-01452-0

Du, G. liang, Zhang, Y. shuang, Iqbal, J., Yang, Z. hua, & Yao, X. (2017). Landslide susceptibility mapping using an integrated

Article DOI: https://doi.org/10.37284/eajenr.7.1.2008

model of information value method and logistic regression in the Bailongjiang watershed, Gansu Province, China. *Journal of Mountain Science*, *14*(2), 249–268. https://doi.org/10.1007/s11629-016-4126-9

Gill, J. C., & Malamud, B. D. (2014). Reviewing and visualizing the interactions of natural hazards. *Reviews of Geophysics*, *52*(4), 680–722. https://doi.org/10.1002/2013RG000445

Guo, C., Montgomery, D. R., Zhang, Y., Wang, K., & Yang, Z. (2015). Quantitative assessment of landslide susceptibility along the Xianshuihe fault zone, Tibetan Plateau, China. *Geomorphology*, *248*, 93–110. https://doi.org/10.1016/j.geomorph.2015.07.012

Hidayat, S., Pachri, H., & Alimuddin, I. (2019). Analysis of Landslide Susceptibility Zone using Frequency Ratio and Logistic Regression Method in Hambalang, Citeureup District, Bogor Regency, West Java Province. *IOP Conference Series: Earth and Environmental Science*, *280*(1), 0–11. https://doi.org/10.1088/1755-1315/280/1/012005

Hong, H., Xu, C., & Bui, D. T. (2015). Landslide Susceptibility Assessment at the Xiushui Area (China) Using Frequency Ratio Model. *Procedia Earth and Planetary Science*, *15*, 513–517. https://doi.org/10.1016/j.proeps.2015.08.065

Ilunga, L. (1991). Morphologie, volcanisme et sedimentation dans le rift du Sud-Kivu. *Bulletin - Societe Geographique de Liege*, *27*, 209–228.

Ilunga, L. (2006). Study the main sites of erosion in Uvira (D.R. Congo). *Geo-Eco-Trop*, *30*(2), 1–12.

Jacobs, L., Dewitte, O., Poesen, J., Maes, J., Mertens, K., Sekajugo, J., & Kervyn, M. (2017). Landslide characteristics and spatial distribution in the Rwenzori Mountains, Uganda. *Journal of African Earth Sciences*, *134*, 917–930. https://doi.org/10.1016/j.jafrearsci.2016.05.013

Kannan, M., Saranathan, E., & Anabalagan, R. (2013). Landslide vulnerability mapping using frequency ratio model: A geospatial approach in Bodi-Bodimettu Ghat section, Theni district, Tamil Nadu, India. *Arabian Journal of Geosciences*, *6*(8), 2901–2913. https://doi.org/10.1007/s12517-012-0587-5

Khan, H., Shafique, M., Khan, M. A., Bacha, M. A., Shah, S. U., & Calligaris, C. (2019). Landslide susceptibility assessment using Frequency Ratio, a case study of northern Pakistan. *Egyptian Journal of Remote Sensing and Space Science*, *22*(1), 11–24. https://doi.org/10.1016/j.ejrs.2018.03.004

Kirschbaum, D. B., Adler, R., Hong, Y., Kumar, S., Peters-Lidard, C., & Lerner-Lam, A. (2012). Advances in landslide nowcasting: Evaluation of a global and regional modeling approach. *Environmental Earth Sciences*, *66*(6), 1683–1696. https://doi.org/10.1007/s12665-011-0990-3

Knapen, A., Kitutu, M. G., Poesen, J., Breugelmans, W., Deckers, J., & Muwanga, A. (2006). Landslides in a densely populated county at the footslopes of Mount Elgon (Uganda): Characteristics and causal factors. *Geomorphology*, *73*(1–2), 149–165. https://doi.org/10.1016/j.geomorph.2005.07.004

Larsen, I. J., & Montgomery, D. R. (2012). Landslide erosion coupled to tectonics and river incision. *Nature Geoscience*, *5*(7), 468–473. https://doi.org/10.1038/ngeo1479

Lee, S., & Pradhan, B. (2007). Landslide hazard mapping at Selangor, Malaysia using frequency ratio and logistic regression models. *Landslides*, *4*(1), 33–41. https://doi.org/10.1007/s10346-006-0047-y

Lepore, C., Kamal, S. A., Shanahan, P., & Bras, R. L. (2012). Rainfall-induced landslide susceptibility zonation of Puerto Rico. *Environmental Earth Sciences*, *66*(6), 1667–

Article DOI: https://doi.org/10.37284/eajenr.7.1.2008

1681. https://doi.org/10.1007/s12665-011-0976-1

Mandal, B., & Mandal, S. (2018). Analytical hierarchy process (AHP) based landslide susceptibility mapping of Lish river basin of eastern Darjeeling Himalaya, India. *Advances in Space Research*, *62*(11), 3114–3132. https://doi.org/10.1016/j.asr.2018.08.008

Maki, J. M., Monsieurs, E., Jacobs, L., & Mateso, L. B. (2016). A regional inventory of the landslide processes and the elements at risk on the Rift flanks west of Lake Kivu (DRC). *Geophysical Research Abstracts*, *18*(April), 6345.

Maki, J. M., & Olivier, D. (2014). Towards an inventory of landslide processes and the elements at risk on the Rift flanks West of Lake Kivu (DRC). *Geo-Eco-Trop*, *18*(January), 137–154.

Migombano Useni, P. (2011). *Évaluation et cartographie par SIG du risque lié aux glissements de terrain à Bukavu (Sud Kivu, RD CONGO)*. 61.

Mohammady, M., Pourghasemi, H. R., & Pradhan, B. (2012). Landslide susceptibility mapping at Golestan Province, Iran: A comparison between frequency ratio, Dempster-Shafer, and weights-of-evidence models. *Journal of Asian Earth Sciences*, *61*, 221–236. https://doi.org/10.1016/j.jseaes.2012.10.005

Mölsä, H., Reynolds, J. E., Coenen, E. J., & Lindqvist, O. V. (1999). Fisheries research towards resource management on Lake Tanganyika. *Hydrobiologia*, *407*, 1–24. https://doi.org/10.1023/A:1003712708969

Moore, R. R. (1978). Rainfall Erosivity in East Africa: Kenya, Tanzania and Uganda. Geografika Annaler. Series A. Physical Geography. 1979. 61; 147-156. *Geografika Annaler. Series A. Physical Geography*, *61*, 147–156.

Mugaruka Bibentyo, T. (2018). *Distribution des glissements de terrain dans un environnement en mutation: Focus sur la gorge de la Ruzizi située entre la RD Congo et le Rwanda*. 66.

Nacishali Nteranya, J. (2021a). Cartographie de l'érosion hydrique des sols et priorisation des mesures de conservation dans le territoire d'Uvira (République démocratique du Congo). *VertigO, Volume 20 Numéro 3*. https://doi.org/10.4000/vertigo.28888

Nacishali Nteranya, J. (2021b). Cartographie de l'érosion hydrique des sols et priorisation des mesures de conservation dans le territoire d'Uvira (République démocratique du Congo). *VertigO, Volume 20 numéro 3*, 1–33. https://doi.org/10.4000/vertigo.28888

Ozer, P. (2009). *Introduction aux risques naturels*. http://orbi.ulg.be/handle/2268/22442

Park, N. W. (2011). Application of Dempster-Shafer theory of evidence to GIS-based landslide susceptibility analysis. *Environmental Earth Sciences*, *62*(2), 367–376. https://doi.org/10.1007/s12665-010-0531-5

Park, S., Choi, C., Kim, B., & Kim, J. (2013). Landslide susceptibility mapping using frequency ratio, analytic hierarchy process, logistic regression, and artificial neural network methods at the Inje area, Korea. *Environmental Earth Sciences*, *68*(5), 1443–1464. https://doi.org/10.1007/s12665-012-1842-5

Persichillo, M. G., Bordoni, M., & Meisina, C. (2017). The role of land use changes in the distribution of shallow landslides. *Science of the Total Environment*, *574*, 924–937. https://doi.org/10.1016/j.scitotenv.2016.09.125

Pimiento, E. (2010). *Shallow Landslide Susceptibility Modelling and Validation*. *6*, 119.

Article DOI: https://doi.org/10.37284/eajenr.7.1.2008

Rabby, Y. W., & Li, Y. (2020). Landslide susceptibility mapping using integrated methods: A case study in the chittagong hilly areas, bangladesh. *Geosciences (Switzerland)*, *10*(12), 1–26. https://doi.org/10.3390/geosciences10120483

Rossi, M., & Reichenbach, P. (2016). LAND-SE: A software for statistically based landslide susceptibility zonation, version 1.0. *Geoscientific Model Development*, *9*(10), 3533–3543. https://doi.org/10.5194/gmd-9-3533-2016

Roy, J., & Saha, S. (2019). Landslide susceptibility mapping using knowledge driven statistical models in Darjeeling District, West Bengal, India. *Geoenvironmental Disasters*, *6*(1). https://doi.org/10.1186/s40677-019-0126-8

Saley, M. B., Kouamé, F. K., Penven, M. J., Biémi, J., & Boyossoro Kouadio, H. (2005). Cartographie Des Zones À Risque D ' Inondation Dans La Région Semi-Montagneuse À Louest De La Côte D ' Ivoire : Apports Des Mna Et De L ' Imagerie Satellitaire. *Télédétection*, *5*(1-2–3), 53–67.

Shafique, M., van der Meijde, M., & Khan, M. A. (2016). A review of the 2005 Kashmir earthquake-induced landslides; from a remote sensing prospective. *Journal of Asian Earth Sciences*, *118*, 68–80. https://doi.org/10.1016/j.jseaes.2016.01.002

Silalahi, F. E. S., Pamela, Arifianti, Y., & Hidayat, F. (2019). Landslide susceptibility assessment using frequency ratio model in Bogor, West Java, Indonesia. *Geoscience Letters*, *6*(1). https://doi.org/10.1186/s40562-019-0140-4

Solaimani, K., Mousavi, S. Z., & Kavian, A. (2013). Landslide susceptibility mapping based on frequency ratio and logistic regression models. *Arabian Journal of Geosciences*, *6*(7), 2557–2569. https://doi.org/10.1007/s12517-012-0526-5

Xiao, J., & Moody, A. (2005). A comparison of methods for estimating fractional green vegetation cover within a desert-to-upland transition zone in central New Mexico, USA. *Remote Sensing of Environment*, *98*(2–3), 237–250. https://doi.org/10.1016/j.rse.2005.07.011

Xu, C., Xu, X., Dai, F., & Saraf, A. K. (2012). Comparison of different models for susceptibility mapping of earthquake triggered landslides related with the 2008 Wenchuan earthquake in China. *Computers and Geosciences*, *46*, 317–329. https://doi.org/10.1016/j.cageo.2012.01.002

Yalcin, A., Reis, S., Aydinoglu, A. C., & Yomralioglu, T. (2011). A GIS-based comparative study of frequency ratio, analytical hierarchy process, bivariate statistics and logistics regression methods for landslide susceptibility mapping in Trabzon, NE Turkey. *Catena*, *85*(3), 274–287. https://doi.org/10.1016/j.catena.2011.01.014

Yilmaz, I. (2010). Comparison of landslide susceptibility mapping methodologies for Koyulhisar, Turkey: Conditional probability, logistic regression, artificial neural networks, and support vector machine. *Environmental Earth Sciences*, *61*(4), 821–836. https://doi.org/10.1007/s12665-009-0394-9

Zamukulu, P. (2020). Susceptibilité des sols d'Idjwi aux risques d'érosion hydrique et glissement de terrain, R.D. Congo. In *Mémoire Master, inédit, Faculté des Sciences Agronomiques et de l'Environnement, UEA Dans* (Issue 1).

